Generation of Isolated Attosecond Pulses with 20 to 28 Femtosecond Lasers

Ximao Feng, Steve Gilbertson, Hiroki Mashiko, He Wang, Sabih D. Khan, Michael Chini,
Yi Wu, Kun Zhao, and Zenghu Chang*

J. R. Macdonald Laboratory, Department of Physics, Kansas State University, Manhattan, Kansas 66506, USA

Isolated attosecond pulses are powerful tools for exploring electron dynamics in matter. So far, such extreme ultraviolet pulses have only been generated using high power, few-cycle lasers, which are very difficult to construct and operate. We propose and demonstrate a technique called generalized double optical gating for generating isolated attosecond pulses with 20 fs lasers from a hollow-core fiber and 28 fs lasers directly from an amplifier. These pulses, generated from argon gas, are measured to be 260 and 148 as by reconstructing the streaked photoelectron spectrograms. This scheme, with a relaxed requirement on laser pulse duration, makes attophysics more accessible to many laboratories that are capable of producing such multicycle laser pulses.

When atoms are driven by laser pulses containing multiple optical cycles, a train of attosecond pulses can be generated [1]. The separation between adjacent pulses is half an optical cycle, which is 1.3 fs for Ti:sapphire lasers. Pulse trains with such a short interpulse spacing have limited use in pump-probe experiments. Instead, isolated attosecond pulses are highly desirable. Since single isolated attosecond pulses were first generated in 2001 [2], they have been used in studying electron dynamics in gaseous atoms [3], in molecules, and in condensed-matter systems [4]. Direct measurement and control of electron motion using such pulses is key to furthering our understanding of matter on as-yet unprecedented time scales. However, generation of isolated attosecond pulses is technically difficult because of the stringent requirements on the driving laser, and so far all experiments using such pulses have been performed in only a few laboratories.

The shortest isolated pulses of 80 as were produced with amplitude gating by <4 fs laser pulses [5]. Another technique to obtain single attosecond pulses is polarization gating [6,7], with which 130-as single attosecond pulses were produced [8]. Several other schemes of generating isolated attosecond pulses using longer laser pulses have been proposed and the extreme ultraviolet (XUV) power spectra were studied, but the durations of the pulses have not been measured [9–11]. The requirement of carrier-envelope (CE) phase stabilized driving lasers with pulse durations of 5 fs or less is one of the main obstacles which has prevented the rapid spreading of attosecond optical technologies. In this Letter, we report generation of single attosecond pulses from 20 to 28 fs laser pulses with a generalized double optical gating (GDOG) method.

Previously we proposed double optical gating (DOG) for generating single attosecond pulses from ~10 fs lasers, which is a combination of polarization gating and two-color gating [11]. The laser field for polarization gating can be resolved into two orthogonally polarized components as shown in Fig. 1(a). The driving field generates the atto-

second pulse, whereas the gating field suppresses the attosecond emission outside of the polarization gate [12]. They can be produced by two counterrotating circularly polarized pulses with a certain delay [13]. Because of the effect of the two-color gating, the polarization gate width should be close to 1 laser cycle to allow only one attosecond emission. However, there is an upper limit on the duration of the input laser pulse. If the laser pulse is too long, the atoms will be fully ionized by the leading edge, leaving no atoms to emit attosecond pulses inside the polarization gate.

To loosen the requirement for the laser pulse duration more, we need to reduce the ground state population depletion from the leading edge of the laser pulse even further. The idea is to create a polarization gating field with
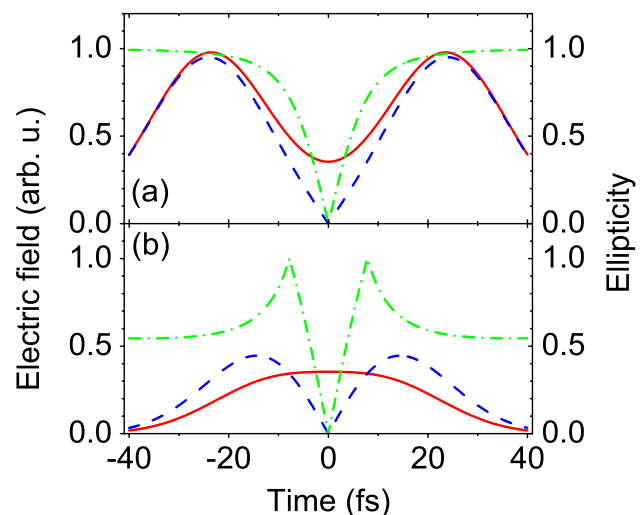

FIG. 1 (color online). Comparison of laser field components for polarization gating in DOG (a) and GDOG (b). In both (a) and (b), the driving field and gating field are plotted in the solid red line and dashed blue line, respectively, and the ellipticity is plotted in the dash-dotted green line.

two counterrotating *elliptically* polarized pulses with an ellipticity, ε [10,12] and a delay T_d, which is a generalization of double optical gating. In this case, the field components are shown in Fig. 1(b). By following the approach in [13], it can be shown that the polarization gate width δt_G can be expressed as

$$\delta t_G \simeq \varepsilon \frac{\xi_{\text{th}}}{\ln(2)} \frac{\tau_p^2}{T_d}, \qquad (1)$$

where ξ_{th} is the threshold ellipticity and τ_p is the laser duration. Here we choose $\xi_{\text{th}} = 0.2$, for which the intensity of attosecond pulses generated outside of the gate is expected to be at least 10 times lower than that of the isolated main pulse. As an example, for 20 fs lasers, δt_G equal to one optical cycle can be obtained by two combinations, i.e., $\varepsilon = 1$ (DOG) and $T_d \simeq 48$ fs or $\varepsilon = 0.5$ (GDOG) and $T_d \simeq 24$ fs as shown in Figs. 1(a) and 1(b). The driving field amplitude inside the gate was kept the same for the two cases. Because the field strength before the gate is lower for GDOG than for DOG, longer laser pulse durations can be used when the intensity at $t = 0$ is the same in both configurations. In general, longer lasers can be used for smaller ε. However, if the ε is too small, attosecond pulses are generated outside of the gate [12].

The attosecond pulses were first generated from argon gas using 20 fs laser pulses for $\varepsilon = 0.5$. In the experiment, 35 fs pulses centered at 790 nm were generated using a Ti:sapphire amplifier operated at 1 kHz. The CE phase of the chirped pulse amplifier (CPA) was stabilized to within 180 mrad rms [14]. The average power of the laser was also locked to 0.5% [15]. The output beam was sent to a gas-filled hollow-core fiber for spectral broadening. The output laser pulse duration was tuned by controlling the gas pressure. Chirped mirrors were used to compensate the

chirp of the laser pulse from the fiber and the dispersion of the optical components. The pulse duration corresponding to the location of the attosecond generation gas target was measured to be 20 fs by frequency-resolved optical gating.

The laser field for GDOG was created using birefringent optics as shown in Fig. 2. A linearly polarized pulse from the laser was incident on the first quartz plate, which had its optical axis oriented at 45° with respect to the input polarization. This created two orthogonally polarized pulses with a delay T_d between them. The combination of the second quartz plate and a type I phase-matched barium borate (BBO) crystal, with their optical axes set in the plane of the input polarization, act as a quarter wave plate. This yielded the two counterrotating fields with a second harmonic field that was polarized parallel to the driving field. Finally, to set $\varepsilon = 0.5$ for the 20 fs laser, a fused silica Brewster window was added. It rejected about 50% of the driving field while leaving the gating field unchanged. The thickness of the first quartz plate was chosen to set T_d to 9 laser cycles for the 20 fs laser pulses.

The isolated XUV pulses were measured using the CRAB (Complete Reconstruction of Attosecond Bursts) method based on attosecond streaking [16,17]. A Mach-Zehnder interferometer configuration was used to control the temporal and the spatial overlap of the attosecond XUV field and the near infrared (NIR) streaking field, as shown in Fig. 2(b). The interferometer stability was locked to 8 as rms using a feedback control.

After the GDOG optics, the 20-fs laser pulse with 0.55 mJ energy was focused to an argon gas target to generate the attosecond XUV pulses. The XUV beam passed through an Al filter and was focused to the detection neon gas target by a multilayer Mo/Si mirror for the
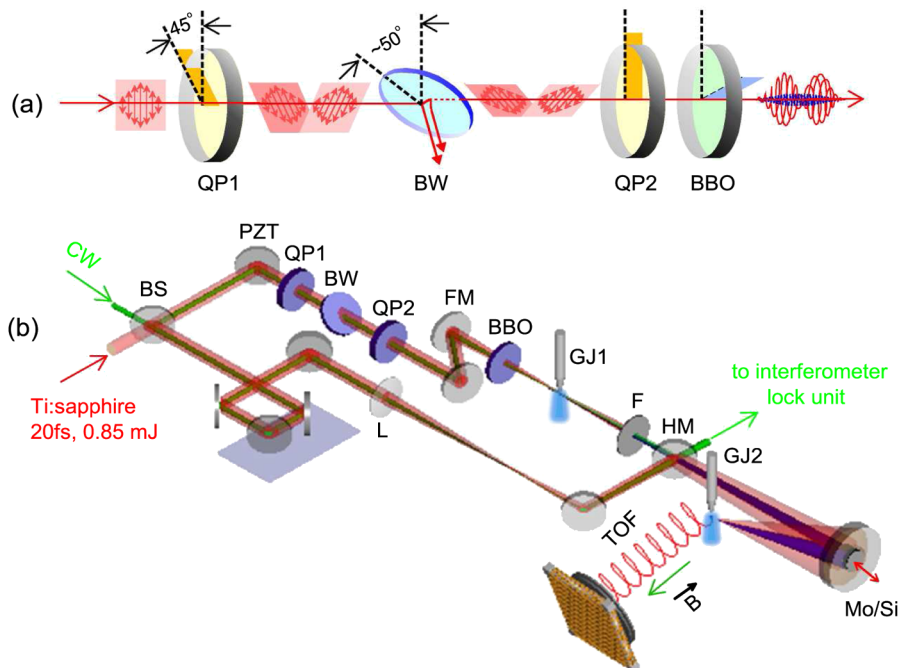

FIG. 2 (color online).   (a) GDOG optics consist of a quartz plate (QP1), a Brewster window (BW), a second quartz plate (QP2), and a BBO crystal. (b) Setup for measuring the single attosecond pulses. The Ti:sapphire laser beam was split into two. One beam propagated through the GDOG optics and was focused by a mirror (M) onto the argon gas jet (GJ1) to generate the attosecond pulses. The aluminum filter (F) filtered out the lower high harmonics and the fundamental beam. The XUV beam was focused by the Mo/Si mirror in the center of the two-component mirror on the detection neon gas target (GJ2). The other beam for streaking traveled through a lens (L) and was focused by the annular mirror in the two-component mirror onto the detection gas jet. The photoelectron energy was measured by a time-of-flight spectrometer (TOF).

production of photoelectrons. The pulse energies of the attosecond pulses before the Al filter were 230 pJ from the 20 fs lasers, measured with an XUV photodiode. Harmonic orders below 30 eV are not transmitted due to absorption by the residual argon gas between the harmonic generation cell and the Al filter and are not included in the energy measurement.

The mirror that combined the XUV beam and the NIR streaking beam had a hole in the center to allow the XUV field to pass through. The streaking laser beam was reflected from the mirror and sent to a curved Ag-coated annular mirror that was concentric to the multilayer mirror. The NIR beam was focused onto the detection gas target where it overlapped with the focused XUV beam.

The time delay between the XUV pulse and the NIR streaking pulse was scanned by moving the XUV mirror with a closed-loop piezoelectric transducer stage. The photoelectron momentum was measured by a time-of-flight spectrometer with a position sensitive delay-line detector. A uniform magnetic field was applied along the flight axis to increase the acceptance angle to 28°. The resolution was better than 0.53 eV for 17 eV electrons.

Figures 3(a) and 3(b) show the experimental and retrieved CRAB traces. Figure 3(c) shows the temporal shape and phase of the 260 as XUV pulse. The frequency marginal comparison shows good agreement as indicated in Fig. 3(d). The minor modulation in the spectrogram comes from the attosecond pre- and postpulses. However, their intensities were 3 orders of magnitude lower than the main pulse, as shown in the inset of Fig. 3(c). Here, from the reconstructed streaking field the NIR intensity was estimated to be 2.8×10^{11} W/cm^2 at the second gas target. Although this intensity is not sufficient to shift the photoelectron spectrum by an amount equal to its bandwidth [17], we have performed numerical simulations which show that such large streaking intensity is not necessary for an accurate CRAB reconstruction [18].

We also generated single attosecond pulses from argon gas with lasers directly from the chirped pulse amplifier. In

this case, the 28 fs laser pulses with 1.5 kHz repetition rate and 1.2 mJ energy after the grating compressor directly were sent to the experimental setup in Fig. 2. The duration of the laser pulse from the amplifier was reduced from 35 fs to 28 fs by adding a spectrum modulator that introduces a larger loss near the center wavelength than that in the wings of the spectrum to counteract the gain narrowing [19]. Based on the angle that the Brewster window was set to in the experiments, ellipticity ε was estimated to be 0.65. The thickness of the first quartz plate was increased so that the delay was 47 fs which gave a gate width of 3.2 fs for 28 fs pulses. We chose these parameters to avoid complete depletion of the ground state population by the field prior to the polarization gate. In this case, the gate width is slightly larger than 1 laser optical cycle.

The results from the CRAB measurements are plotted in Fig. 4. The retrieval procedure and the plot format are exactly the same as those for Fig. 3. The retrieved pulse duration was 148 as, which is longer than the transform-limited value, 131 as, due to the residual phase error. The pre- and postpulses were less than 1% of the main pulse when the effects of the energy resolution were taken into account. The good match of the XUV-only spectrum to the retrieved XUV spectrum as shown in Fig. 4(d) indicates the validity of the retrieval.

The CRAB technique has been previously demonstrated as an effective tool for the measurement of isolated attosecond pulses [16] and for attosecond pulses with satellite pulses with half-cycle [20] and full-cycle [21] periodicity. However, the CRAB traces from attosecond streaking experiments can be degraded by shot noise and spectral resolution. These issues will most significantly affect the detection of satellite pre- and postpulses, which are evident by small modulations in the energy spectrum. In order to determine the severity of these issues on the reconstruction of the satellite pulse contrast, we created CRAB traces numerically with shot noise added and with different detector resolutions. The details of these simulations will be published elsewhere. The conclusions for retrieval of sat-
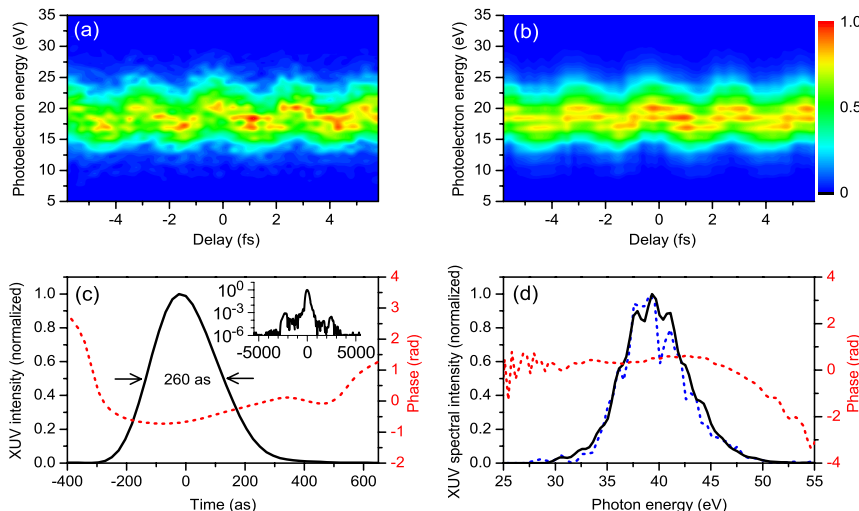

FIG. 3 (color online). Attosecond XUV pulse generated from argon gas using 20 fs laser pulses. (a) Experimental CRAB trace. (b) Retrieved trace. (c) Retrieved XUV pulse (solid line) and temporal phase (dashed line). The inset shows the temporal profile over 4 cycles on a log scale. (d) Comparison of the measured unstreaked XUV spectrum (blue or dark gray dashed line) and the retrieved XUV spectrum (solid line) accompanied by the retrieved spectral phase (red or gray dashed line). A positive chirp of 7850 as^2 was obtained from the phase.
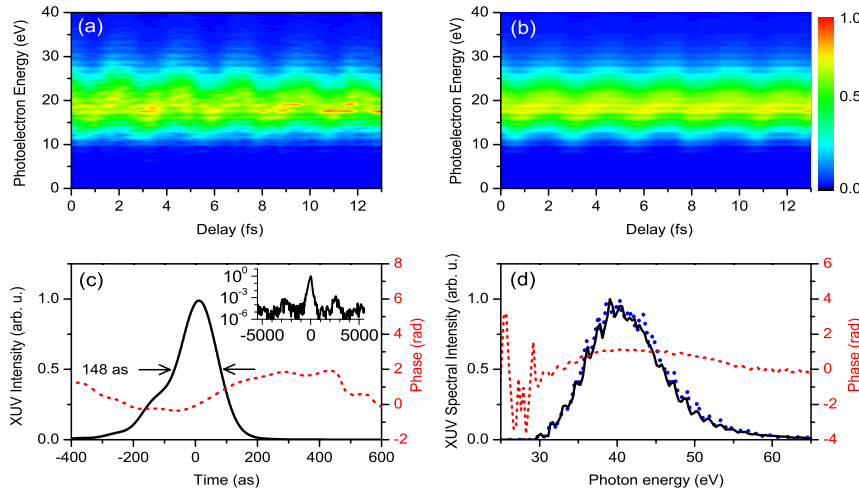
FIG. 4 (color online). Attosecond XUV pulse generated from argon gas using 28 fs laser pulses directly from the amplifier. (a) Experimental CRAB trace. (b) Retrieved CRAB trace. (c) Retrieved XUV pulse (solid line) and temporal phase (dashed line). The inset shows the temporal profile over 4 cycles on a log scale. (d) Comparison of the measured unstreaked XUV spectrum (blue or dark gray dashed line) and the retrieved XUV spectrum (solid line) accompanied by the retrieved spectral phase (red or gray dashed line).

ellite pulses with full-cycle periodicity and relative intensity of 10^{-2} and 10^{-3} are that in the case that the detector resolution is around 0.5 eV, the satellite pulse contrast is underestimated by roughly 60%. When shot noise is present, the satellite pulse contrast can be accurately retrieved when the photoelectron count at the peak of the spectrogram is 200 counts per pixel or greater. When the relative intensity of the satellite pulses is 1% of the main pulse, the modulation in the spectrum has a contrast of more than 50%, which is nearly 10 times larger than the signal-to-noise ratio when shot noise is considered for 200 counts. In contrast, our measured spectrogram typically has a peak count exceeding 1000 counts. Thus the real satellite pulses were less than 1% as intense as the main pulse.

In conclusion, we have generated single isolated attosecond pulses of 260 as with 20 fs multicycle laser pulses from hollow-core fibers and of 148 as with 28 fs amplifier laser pulses, and measured the pulses unambiguously by the CRAB method. The generation of isolated attosecond pulses with such long pulse lasers offers two advantages. First, they are much easier to work with than the fragile ≤5 fs lasers used in previous attosecond generation experiments. Second, their energy can be much higher than the few-cycle lasers, which allows the scaling of isolated attosecond pulses to the energy level needed for studying nonlinear phenomena.

*chang@phys.ksu.edu

[1] P. M. Paul, E. S. Toma, P. Breger, G. Mullot, F. Augé, P. Balcou, H. G. Muller, and P. Agostini, Science **292**, 1689 (2001).

[2] M. Hentschel, R. Kienberger, C. Spielmann, G. A. Reider, N. Milosevic, T. Brabec, P. Corkum, U. Heinzmann, M. Drescher, and F. Krausz, Nature (London) **414**, 509 (2001).

[3] M. Drescher, M. Hentschel, R. Kienberger, M. Uiberacker, V. Yakovlev, A. Scrinzi, T. Westerwalbesloh, U. Kleineberg, U. Heinzmann, and F. Krausz, Nature (London) **419**, 803 (2002).

[4] A. L. Cavalieri et al., Nature (London) **449**, 1029 (2007).

[5] E. Gouliemakis et al., Science **320**, 1614 (2008).

[6] P. B. Corkum, N. H. Burnett, and M. Y. Ivanov, Opt. Lett. **19**, 1870 (1994).

[7] O. Tcherbakoff, E. Mevel, D. Descamps, J. Plumridge, and E. Constant, Phys. Rev. A **68**, 043804 (2003).

[8] G. Sansone et al., Science **314**, 443 (2006).

[9] Y. Oishi, M. Kaku, A. Suda, F. Kannari, and K. Midorikawa, Opt. Express **14**, 7230 (2006).

[10] P. Tzallas, E. Skantzakis, C. Kalpouzos, E. P. Benis, G. D. Tsakiris, and D. Charalambidis, Nature Phys. **3**, 846 (2007).

[11] H. Mashiko, S. Gilbertson, C. Li, S. D. Khan, M. M. Shakya, E. Moon, and Z. Chang, Phys. Rev. Lett. **100**, 103906 (2008).

[12] D. Oron, Y. Silberberg, N. Dudovich, and D. M. Villeneuve, Phys. Rev. A **72**, 063816 (2005).

[13] Z. Chang, Phys. Rev. A **70**, 043802 (2004).

[14] C. Li, E. Moon, and Z. Chang, Opt. Lett. **31**, 3113 (2006).

[15] H. Wang, C. Li, J. Tackett, H. Mashiko, C. M. Nakamura, E. Moon, and Z. Chang, Appl. Phys. B **89**, 275 (2007).

[16] Y. Mairesse and F. Quéré, Phys. Rev. A **71**, 011401(R) (2005).

[17] J. Itatani, F. Quéré, G. L. Yudin, M. Yu. Ivanov, F. Krausz, and P. B. Corkum, Phys. Rev. Lett. **88**, 173903 (2002).

[18] H. Wang, M. Chini, S. D. Khan, S. Chen, S. Gilbertson, X. Feng, H. Mashiko, and Z. Chang, J. Phys. B **42**, 134007 (2009).

[19] V. Bagnoud and F. Salin, Appl. Phys. B **70**, S165 (2000).

[20] J. Gagnon, E. Goulielmakis, and V. S. Yakovlev, Appl. Phys. B **92**, 25 (2008).

[21] M. Chini, H. Wang, S. D. Khan, S. Chen, and Z. Chang, Appl. Phys. Lett. **94**, 161112 (2009).